J. Plant Biol. (2019) 62:274-285
DOI 10.1007/s12374-019-0051-0

ORIGINAL ARTICLE

Formation of Protein Bodies and the Response to Nitrogen in Different Positions During Wheat Endosperm Development

Yang Yang, Xinyu Chen, Liping Ran, Yunfei Wu, Xurun Yu, Zhaodi Dong and Fei Xiong*

Jiangsu Key Laboratory of Crop Genetics and Physiology/Co-Innovation Center for Modern Production Technology of Grain Crops/ Joint International Research Laboratory of Agriculture & Agri-Product Safety, Yangzhou University, Yangzhou 225009, China

Received: February 11, 2019 / Accepted: May 15, 2019
© Korean Society of Plant Biologists 2019

Abstract The development of protein bodies (PBs) determines the processing properties of wheat (*Triticum aestivum* L.). It has been known that nitrogen uptake has a strong impact on grain protein concentration. However, the differences of the formation of PB in different developmental stages and different positions in wheat endosperm are still controversial. To solve these issues, PBs formation in different wheat endosperm parts and the response to nitrogen were investigated using light, transmission electron microscopes in present study. The main results were as follows. (1) Proteins mainly formed PBs via the Golgi apparatus in the vacuole at the early stage of wheat endosperm development. After 7 days post anthesis, most proteins were derived from the rough endoplasmic reticulum. (2) The morphology of PBs was diverse among different endosperm parts. Compared with the central endosperm, the PBs in sub-aleurone cells were abundant and large. (3) More abundant endoplasmic reticulum, Golgi and mitochondrion were observed at the early stage after nitrogen treatment. Nitrogen also increased the accumulation of PBs at the later stage. (4) The sub-aleurone region cells of the endosperm presented more significant responses to nitrogen than the central endosperm.

Keywords: Development, Endosperm, Nitrogen, Protein body, Wheat

Introduction

Wheat (*Triticum aestivum* L.) is one of the most important cereal crops in the world. The endosperm makes up more than 85% of wheat grain in weight, which accumulates protein and starch during caryopsis development. Composition and concentration of grain protein are major elements for grain nutritional value, as well as for flour functional properties (Martre 2003; Tosi et al. 2011). Glutenin and gliadin prolamins are the two group storage proteins of importance, making up 60 to 80% of total grain proteins. Gliadins are monomeric fractions composed of three classes (α-, γ-, and ω-) gliadins (Loussert et al. 2008; Vensel et al. 2018). Glutenins, forming large macropolymers during grain desiccation, have been divided into high molecular weight (HMW) and low molecular weight (LMW) groups based on their separation by SDS-PAGE (Don et al. 2006; Shewry et al. 2009). Protein composition has influence on size and structure of protein polymer. (Vensel et al. 2018). The storage protein, forms a continous visco-elastic network in dough, is closely related to the processing quality (Guo et al. 2012). Rubin et al. (1992) provided evidence for the existence of two different types of protein bodies (PBs) in wheat. The denser PBs appeared to be formed by aggregation of storage proteins within the endoplasmic reticulum (ER) and were enriched both HMW-Glutenin subunits (GS) and gliadins while the lighter PBs, only enriched in gliadins, resulted in aggregation at a post-ER location (the vacuole).

Synthesis, fold and deposition of storage proteins take place within the endosperm membrane system of the plant cells (Tosi et al. 2012). The formation of wheat endosperm PBs has been reported. These studies are in agreement with previous suggestions that two trafficking pathways (Arcalis et al. 2004; Tosi et al. 2009), transported into the protein storage vacuole (PSV) by Golgi apparatus (Bechtel et al. 1982a; Kim et al. 1988; Loussert et al. 2008) or accumulating directly within the lumen of the ER (Rubin et al. 1992; Galili et al. 1995; Kumamaru et al. 2007). The fold and assembly of storage proteins are aided by ER lumenal proteins such as the molecular chaperone binding protein (BiP) (Rubin et al. 1992) and folding enzymes like protein disulphide isomerase (PDI) (Paola et al. 2012; Katarzyna et al. 2018).

It has been known that nitrogen supply has vital effect on

*Corresponding author; Fei Xiong
Tel : +86-514-87979354
E-mail : feixiong@yzu.edu.cn

grain protein content at reproductive stage in wheat, especially at grain filling stage (Kichey et al. 2007; García-Molina et al. 2017). Optimise modified nitrogen use efficiency is considered to promote high content of grain yield and grain protein (Iqtidar et al. 2006; Zhen et al. 2017). Maximum biological yield was observed under application 150 kg hm^{-2} of nitrogen (Iqtidar et al. 2006). The crude protein content increased significantly with increasing N up to 225 kg hm^{-2} and stopped increasing at N 300 kg hm^{-2}. On the contrary, the content of various fibers tended to decrease with the increase of N application (Li et al. 2016). Nitrogen not only affects the accumulation of total protein, but also leads to different protein composition, such as low gliadin and glutenin content (Wang et al. 2003; Wu et al. 2005; Garcíamolina et al. 2017).

Wheat endosperm is generally divided into two parts: sub-aleurone region and central region of endosperm. As the endosperm develops, different positions show different type or concentration of PBs. In general, the PBs of wheat endosperm close to the endosperm cavity is smallest, and then enlarged gradually from the inside to the outside (Normand et al. 1965). HMW and LMW glutenins were observed in outer and inner endosperm using immunofluorescence double labelling (Tosi et al. 2009). Most of the gliadins were present in the light PBs, whereas at more mature stages, they were found in both the light and the dark (Rubin et al. 1992).

Previous studies have presented relevant evidence on the formation of PBs. However, little is known about the spatial distribution characteristics of storage protein accumulation in wheat endosperm and the cytological mechanism of nitrogen treatment. In this study, the formation of wheat endosperm PBs and nitrogen effects in different region cells were investigated by resin slice technology, microstructural and ultrastructural observation. Our study could provide a theoretical basis for high quality wheat cultivars.

Results

PBs Formation of Sub-aleurone Region and the Response to Nitrogen

The microstructure of cells in the sub-aleurone region after

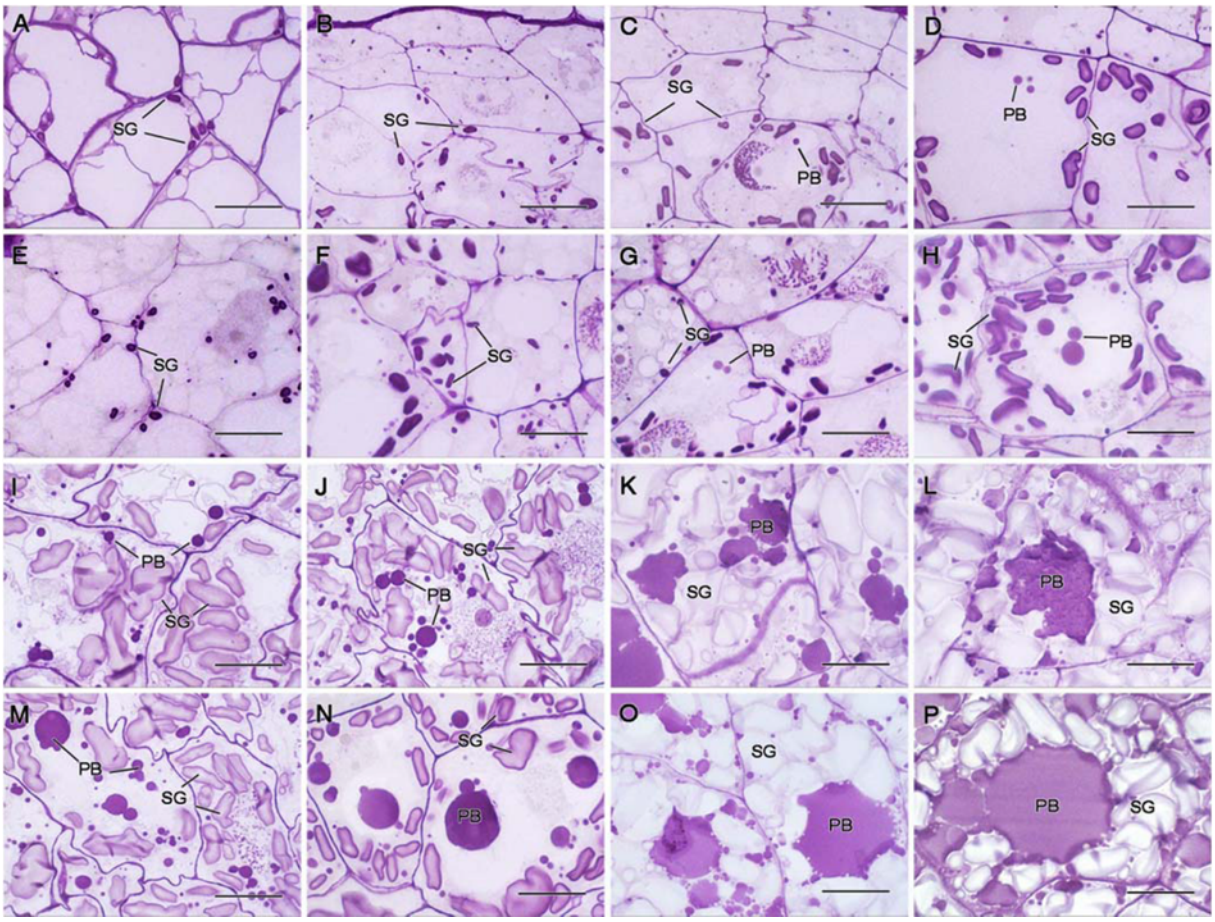

Fig. 1. Microstructure of sub-aleurone region cells after nitrogen treatment. Sub-aleurone region cells of CG (A) at 6 DPA, (B) 7 DPA, (C) 8 DPA, (D) 9 DPA, (I) 10 DPA, (J) 11 DPA, (K) 18 DPA and (L) 24 DPA; Sub-aleurone region cells of NTG (E) at 6 DPA, (F) 7 DPA, (G) 8 DPA, (H) 9 DPA, (M) 10 DPA, (N) 11 DPA, (O) 18 DPA and (P) 24 DPA. SG, Starch granule; PB, protein body. Bars = 100 μm.

nitrogen treatment was shown in Fig. 1. At 6 to 7 days post anthesis (DPA), some starch granules presented in the peripheral cytoplasm, no obvious PBs were detected under a light microscope (Fig. 1A, B, E, F). At 8 DPA, The protein microparticles wrapped with membranes were observed in the vacuoles of the control group (CG) cells (Fig. 1C). In the nitrogen treatment group (NTG), smaller vacuoles were clearly visible (Fig. 1G). And the protein particles began to aggregate, which were larger than that in the CG (Fig. 1C). At 9 DPA, the volume of protein globules both in the CG and the NTG increased, especially in the NTG (Fig. 1D, H).

During the endosperm development, numerous protein globules appeared in the vacuoles. And the volume and number of PBs increased significantly at this stage. At 10 to 11 DPA, abundant spherical storage protein particles of different sizes were observed, which mainly located at the PSV as PBs. In the CG, there were some small protein particles around the large proteins (Fig. 1I, M), whereas the NTG cells contained larger protein deposits formed by the fusion of small protein particles (Fig. 1J, N). At 18 DPA, endosperm cell contained more starch, and more volume of PBs in the CG and NTG were formation. Small PBs of the CG was clustered in a same vacuole with many small particle proteins dispersed around (Fig. 1K). However, the larger PBs or aggregates was formation in endosperm cell under nitrogen treatment (Fig. 1O). At 24 DPA, the storage proteins formed the protein matrix in the sub-aleurone of endosperm, which encapsulated in the starch granules (Fig. 1L, P).

Changes in the Number and Relative Area of PBs in the Sub-aleurone Region of Endosperm after Nitrogen Treatment

The number and relative area of PBs in the sub-aleurone region at different stages of endosperm development were calculated using Image-Pro Plus (Fig. 2). There was no significant difference in the number of PBs between the NTG and the CG at 8 DPA. At 9-10 DPA, the number of PBs was increased both in the CG and the NTG, but the NTG was significantly higher than the CG. The protein globules gradually aggregated into larger volume of PBs from 11 DPA. The number of PBs tended to decrease in the NTG and CG. Compare with CG, the number of PBs in the NTG was less which might due to aggregate earlier (Fig. 2A). During the entire endosperm developmental, the relative area of CG and NTG PBs in the endosperm continued to increase, and the NTG was significantly higher than that in CG (Fig. 2B).

PBs Formation of Central Endosperm Cells and the Response to Nitrogen

Figure 3 showed the microstructure of wheat endosperm central cells. No obvious PBs was observed in the central cells of the CG and NTG at 6 DPA. The starch granules in NTG were more abundant than that in CG, which was surrounded the cell wall (Fig. 3A, E). At 7 DPA, tiny individual protein appeared in the central endosperm region cells of the CG (Fig. 3B), while multiple protein globules were found in the NTG cells (Fig. 3F). At 8 DPA, the accumulation of protein globules could be clearly observed at this time (Fig. 3C, G).

At 9 to 10 DPA, compared with the previous period, the number of PBs increased rapidly with many small particles around the larger protein (Fig. 3D, I, H, M). At 11 to 18 DPA, PBs was more cohesive to the surrounding protein particles, which formed protein deposits and were confined to a certain position by starch granules. This feature was particularly significant in the NTG (Fig. 3J, K, N, O). At 24 DPA, storage proteins were small and mostly spherical, dispersed in the starch granules in different size (Fig. 3L, P).

Changes in the Number and Relative Area of PBs in the Central Endosperm Cells after Nitrogen Treatment

Figure 4 displayed changes in the number and relative area

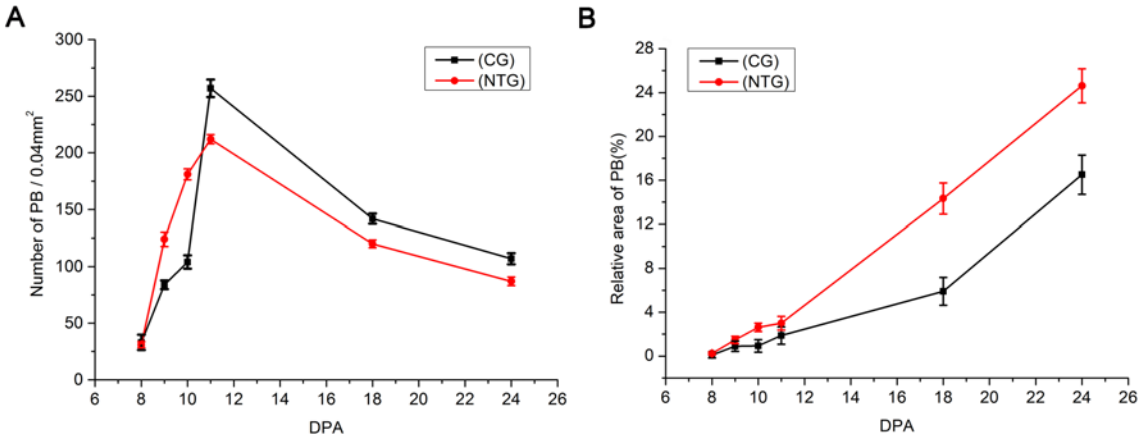

Fig. 2. (A) Number and (B) relative area of PBs in the sub-aleurone region after nitrogen treatment.

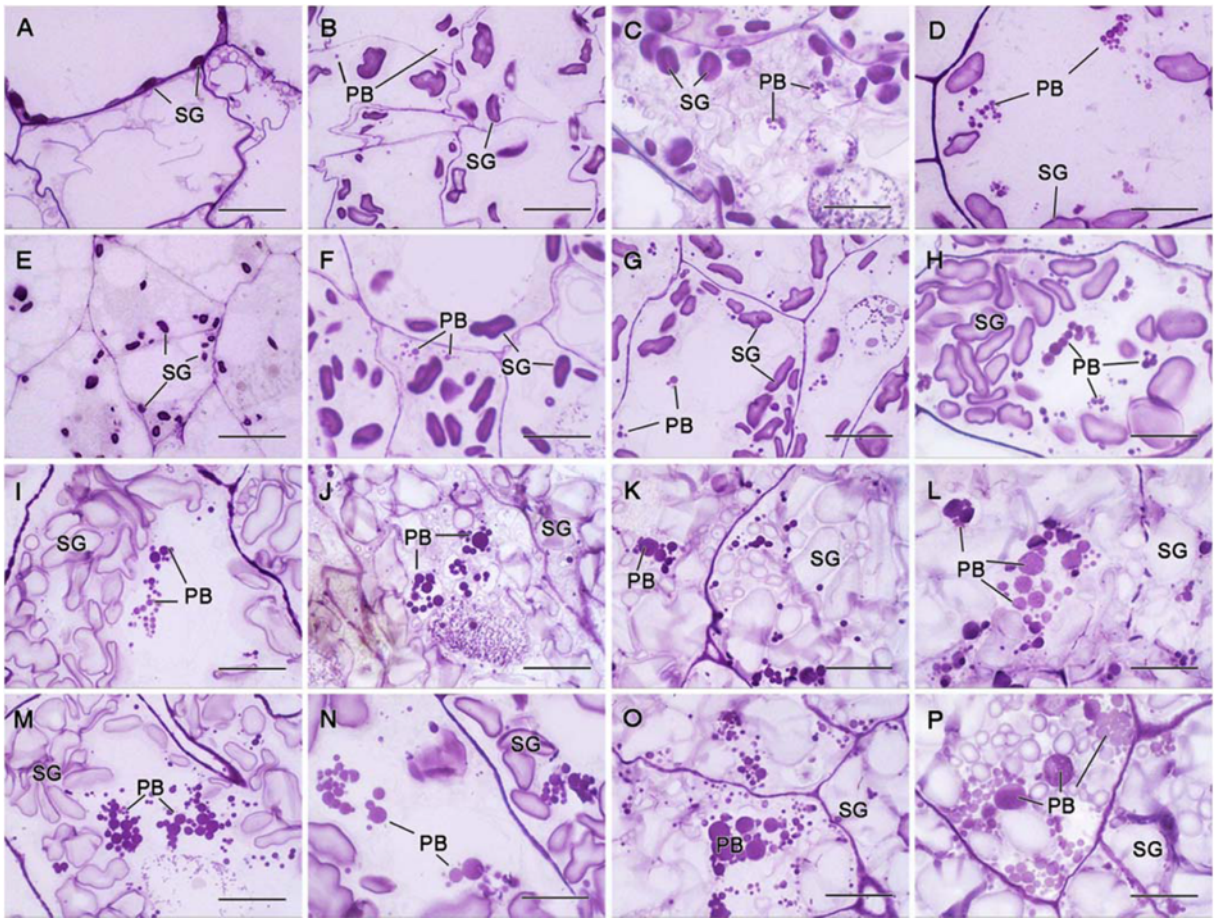

Fig. 3. Microstructure of central endosperm cells after nitrogen treatment. Central endosperm cells of CG (A) at 6 DPA, (B) 7 DPA, (C) 8 DPA, (D) 9 DPA, (I) 10 DPA, (J) 11 DPA, (K) 18 DPA and (L) 24 DPA; Central endosperm cells of NTG (E) at 6 DPA, (F) 7 DPA, (G) 8 DPA, (H) 9 DPA, (M) 10 DPA, (N) 11 DPA, (O) 18 DPA and (P) 24 DPA. SG, Starch granule; PB, Protein body. Bars = 100 μm.

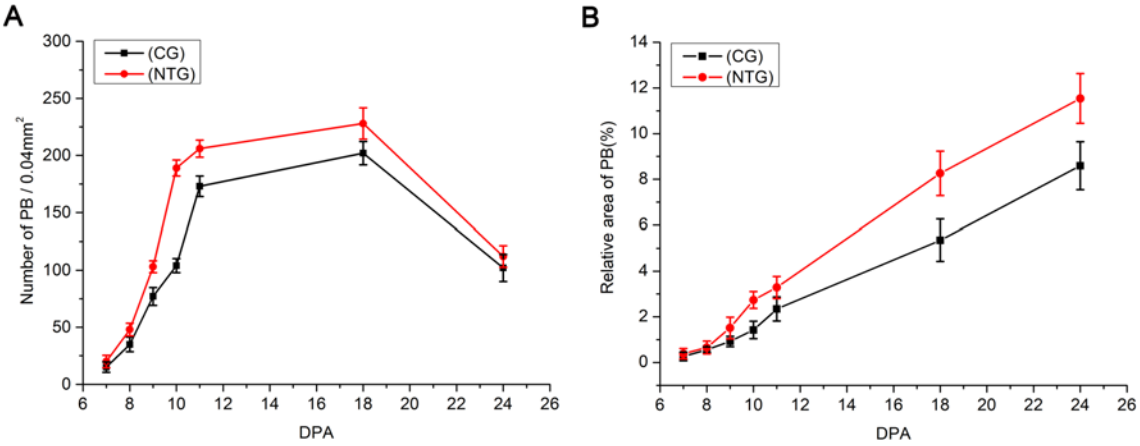

Fig. 4. (A) Number and (B) relative area of PBs in the central endosperm after nitrogen treatment.

of PBs in the central endosperm cells after nitrogen treatment. The figure illustrated that PBs in CG and NTG increased at 8-18 DPA. After 18 DPA, PBs gradually decreased because of the aggregation of protein (Fig. 4A). The number of PBs in the NTG was higher than that in the CG throughout development, which was different from Fig. 2A. The difference caused by that the number of PBs in the sub-aleurone region increased rapidly compared with that in the central endosperm, and also, the PBs at the late stage were more concentrated.

Throughout the developmental process, the relative area of PBs in the central endosperm region cells of NTG was significantly higher than that of the CG (Fig. 4B). Compared

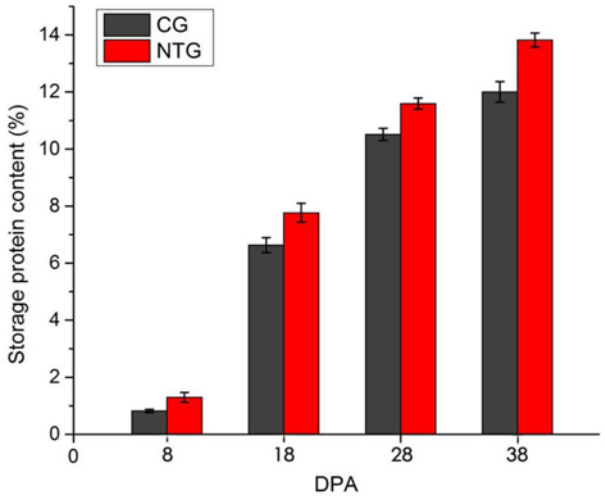

Fig. 5. Storage protein content of caryopses under nitrogen treatment at different developmental stages.

with Fig. 2B, the area of sub-aleurone region protein accumulated faster than that of the central endosperm region cells. The results demonstrated that the response in sub-aleurone region to nitrogen was greater than that in the central endosperm region cells.

Storage Protein Content of Caryopses Under Nitrogen Treatment

As the development of wheat caryopsis, protein content continually roes and reached peak at 38 DPA. At 8 DPA, no significant difference in storage protein content was found between CG and NTG. At 18, 28, 38 DPA (mature stage), the protein content of caryopsis under NTG was constantly higher than control (Fig. 5). The results above indicated that nitrogen treatment significantly enhanced the actual storage protein content, which was consistent with the fact in the

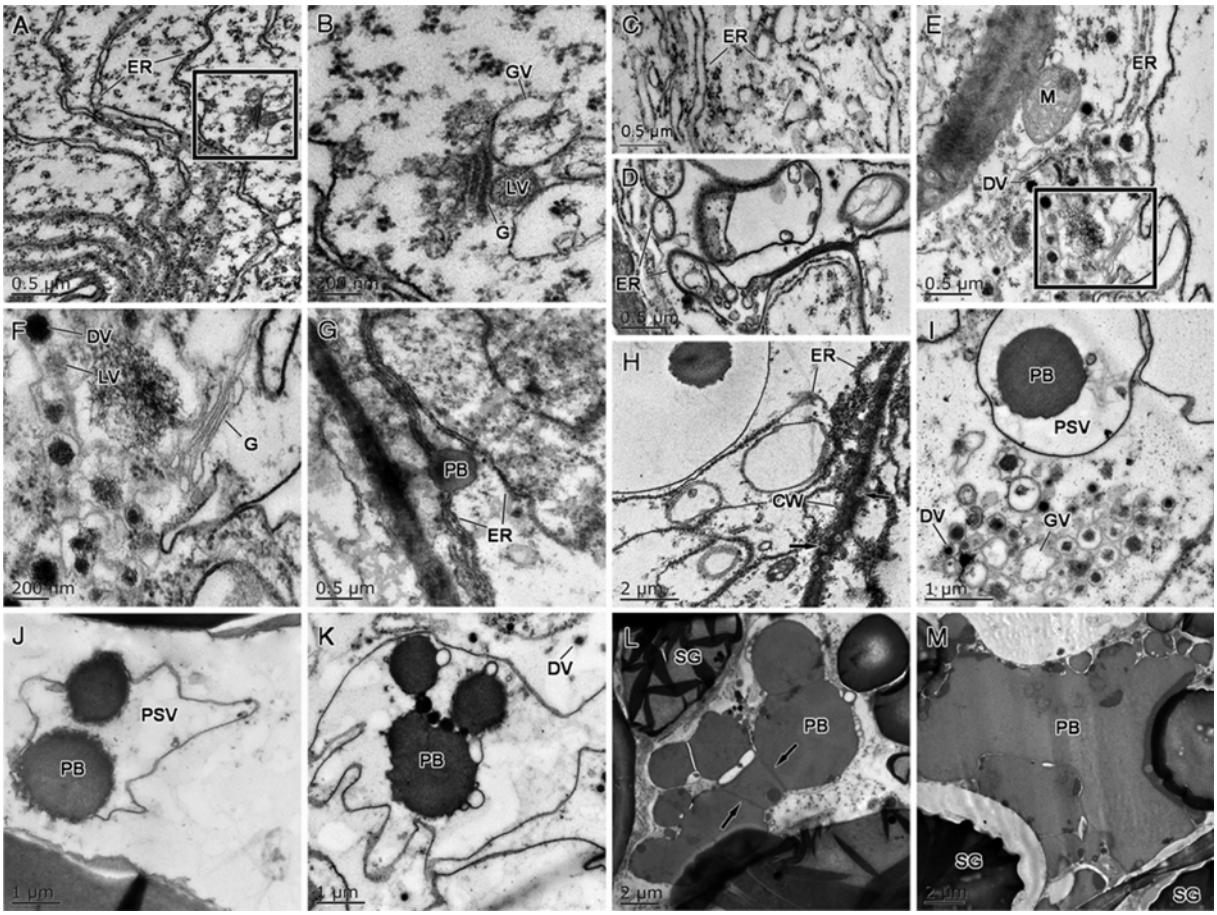

Fig. 6. Formation of PBs during endosperm development. (A) Golgi apparatus and abundant ER in 6 DPA endosperm; (B) Enlargement of box area of Fig. 6A, electron-lucent vesicles and Golgi vacuoles produced by Golgi apparatus; (C) fragmentary ER and (D) circular ER of 7 DPA cells; (E) Vesicles produced by the ER were transported to the Golgi apparatus at 7 DPA; (F) Enlargement of box area of Fig. 6E, electron-lucent vesicles and dense vesicles around the Golgi aparatus; (G) The lumen of the ER enlarged in some points and accumulates protein at 8 DPA; (H) Endosperm 8 DPA that had vesicles fused with plasmalemma and star-shaped inclusions incorporated into cell wall (arrows); (I) Electron-lucent vesicles, dense vesicles and Golgi vacuoles moved close to the vacuole at 9 DPA; (J) At 10 DPA, PBs were entering the PSV; (K) The dense vesicles produced by the Golgi apparatus and the PBs produced by the ER all appeared in the 10 DPA PSV; (L) At 18 DPA, proteins fused with each other, and arrows indicate protein membranes; (M) At 24 DPA, structure of the storage protein matrix. SG, Starch granules; PB, Protein body; DV, Dense vesicles; ER, Endoplasmic reticulum; GV, Golgi vacuoles; LV, Lucent vesicles; M, Mitochondrion; G, Golgi apparatus; CW, Cell wall; PSV, Protein storage vacuole.

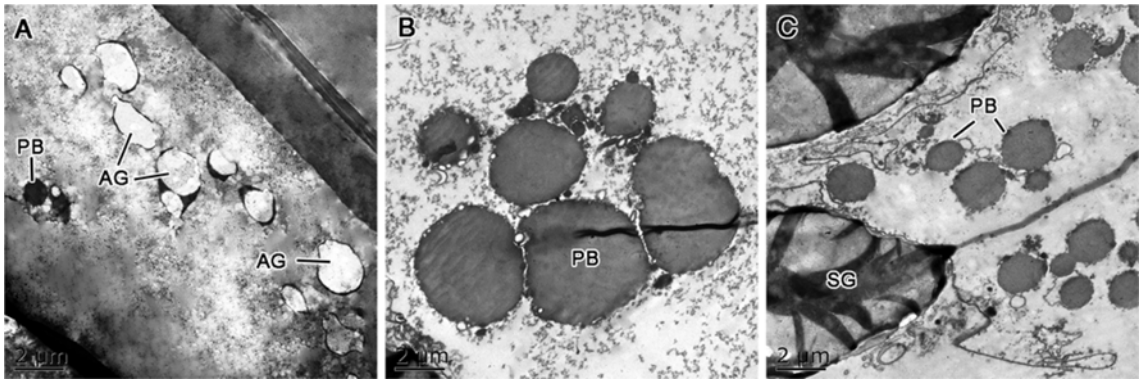

Fig. 7. Ultrastructure of PBs in aleurone layer, sub-aleurone region, and the central cells. (A) Aleurone cells at 11 DPA; (B) Sub-aleurone cells at 11 DPA; (C) Central endosperm region cells at 11 DPA. PB, Protein body; AG, Aleurone granules; SG, Starch granules.

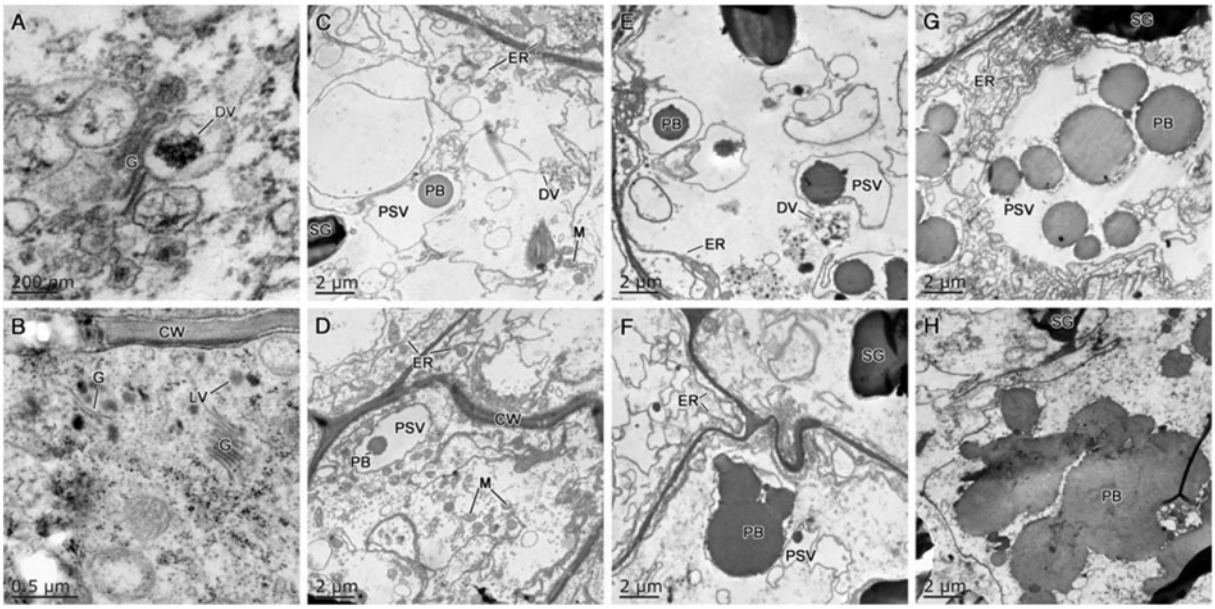

Fig. 8. Ultrastructure of PBs in the sub-aleurone region after nitrogen treatment. Sub-aleurone region cells of CG (A) at 6 DPA, (C) 8 DPA, (E) 9 DPA and (G) 11 DPA. Sub-aleurone region cells of NTG (B) at 6 DPA, (D) 8 DPA, (F) 9 DPA and (H) 11 DPA. SG, Starch granules; PB, Protein body; DV, Dense vesicles; ER, Endoplasmic reticulum; G, Golgi apparatus; M, Mitochondrion; PSV, Protein storage vacuole; CW, Cell wall; LV, Lucent vesicles.

microstructure (Fig. 2; Fig. 4).

PBs Formation

Figure 6 showed the ultrastructure of the endosperm PBs. At 6 DPA, The ER and the Golgi apparatus were visible. At this point, the Golgi was producing electron-lucent vesicles and Golgi vacuoles (Fig. 6A, B). At 7 DPA, the ER varied in fragmentary (Fig. 6C), circular (Fig. 6D) or linear (Fig. 6E) shape. At the same time, the vesicles produced by the ER were transported to the Golgi, Which were often closely associated with the Golgi stacks and surrounded by electron-lucent material enclosed within the membrane (Fig. 6F).

At 8 DPA, the ER seemed to be enlarged in some points to form cisternae, in which the protein was being synthesised (Fig. 6G). Storage proteins would be detached from the ER as the accumulation of storage proteins. Then vesicles fused with plasmalemma and star-shaped inclusions incorporated into cell wall (Fig. 6H). At 9 to 10 DPA, fewer Golgi apparatus were observed at this stage in endosperm cells, the vacuoles in the endosperm cells were distinct. The ER-derived proteins and vesicles produced by the Golgi apparatus gradually got into the vacuoles (Fig. 6I, J). Larger PBs surrounded by small electron-opaque vesicles were observed at 11 DPA, they combined together in the vacuole to form PSV (Fig. 6K).

No Golgi structures with stacked cisternae were visible at 18 DPA. Storage vacuole contained multiple PBs which were close to each other but not completely fused. The arrows in the figure showed a clear boundary between

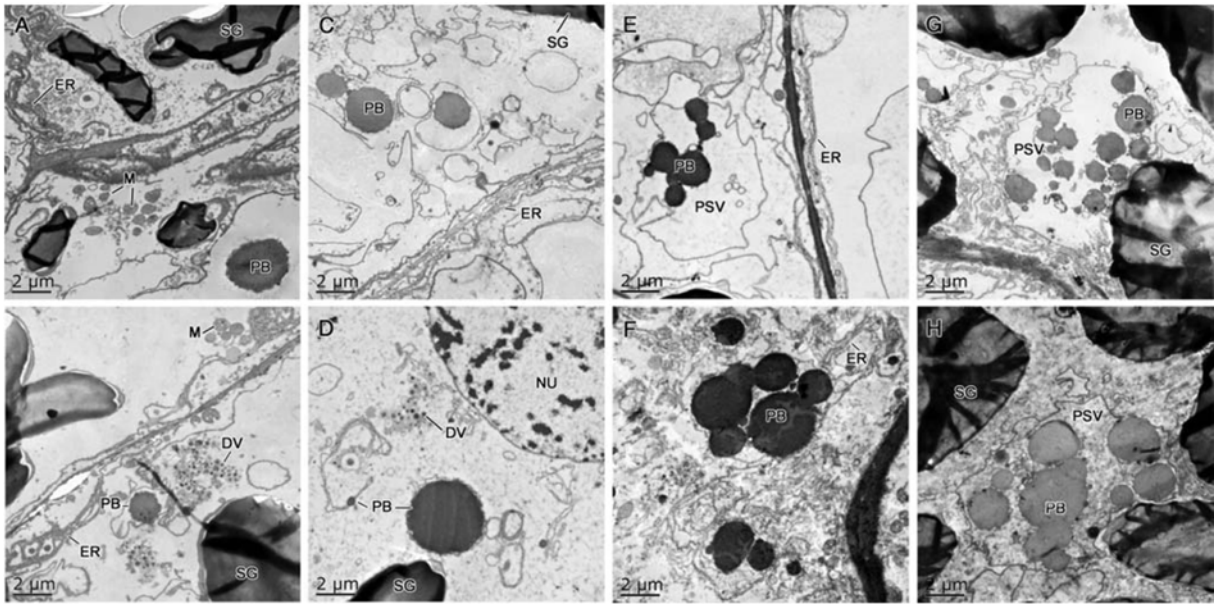

Fig. 9. Ultrastructure of PBs in the central endosperm cells after nitrogen treatment. Central endosperm cells of CG (A) at 8 DPA, (C) 9 DPA, (E) 10 DPA and (G) 11 DPA. Central endosperm cells of NTG (B) at 8 DPA, (D) 9 DPA, (F) 10 DPA and (H) 11 DPA. SG, Starch granules; PB, Protein body; DV, Dense vesicle; ER, Endoplasmic reticulum; G, Golgi apparatus; M, Mitochondrion; PSV, Protein storage vacuole; CW, Cell wall; NU, Nucleus.

proteins (Fig. 6L). At 24 DPA, protein matrix was large, irregular in shape and distributed between the starch granules (Fig. 6M).

Morphology of PBs in the Aleurone Layer, Sub-aleurone Region, and Central Cells of Endosperm

Figure 7 displayed the ultrastructure of PBs in aleurone layer, sub-aleurone region, and the central cell. In aleurone cells, most of the proteins were combined with phytin to form aleurone granules, and fewer of them existed as PBs (Fig. 7A). The PBs in the sub-aleurone cells were large in volume and small in number, and some of them combined to form large protein aggregates (Fig. 7B). The central endosperm cells were small but rich in PBs. Most of the PBs was distributed loosely (Fig. 7C).

Ultrastructure of PBs in the Sub-aleurone Region after Nitrogen Treatment

Figure 8 displayed the ultrastructure of PBs in the sub-aleurone region after nitrogen treatment. At 6 to 8 DPA, sub-aleurone cells were rich in Golgi, rough ER, PSV and mitochondria, and it was more distinct in the NTG (Fig. 8A, B, C, D). At 9 DPA, small proteins of NTG were fused with large PBs in the PSV, and the PBs development progress was faster than that in the CG (Fig. 8E, F). At 11 DPA, Many PBs in PSV was observed. The large protein formed by the fusion of PBs in the NTG deposited in the cytoplasm (Fig. 8G, H).

Ultrastructure of PBs in the Central Region Cells after Nitrogen Treatment

Figure 9 showed the ultrastructure of wheat central endosperm region cells after nitrogen treatment. 8 to 9 DPA was the active period of protein synthesis. A large number of ER was existed in the CG (Fig. 9A, C) and dense vesicles produced by the Golgi apparatus were observed in the NTG (Fig. 9B, D). At 10 to 11 DPA, more and more proteins appeared in the PSV (Fig. 9E, F).

Discussion

Formation of the PBs

The early phase of wheat grain development mainly involved active cell enlargement, leading to a rapid increase in seed size available for further accumulation of storage proteins (Yang et al. 2016). The occurrence and accumulation of PBs were related to the characteristics of varieties, temperature, and other factors (Guo et al. 2012; Savill et al. 2018). In present study, PBs occurred in the sub-aleurone cells as early as 7 DPA. At the early stages of caryopsis development, PBs was spherical with diameters around 1 to 2 mm and the endosperm cells contained large protein deposits formed by the fusion of small PBs (Moore et al. 2016). Later, around 10

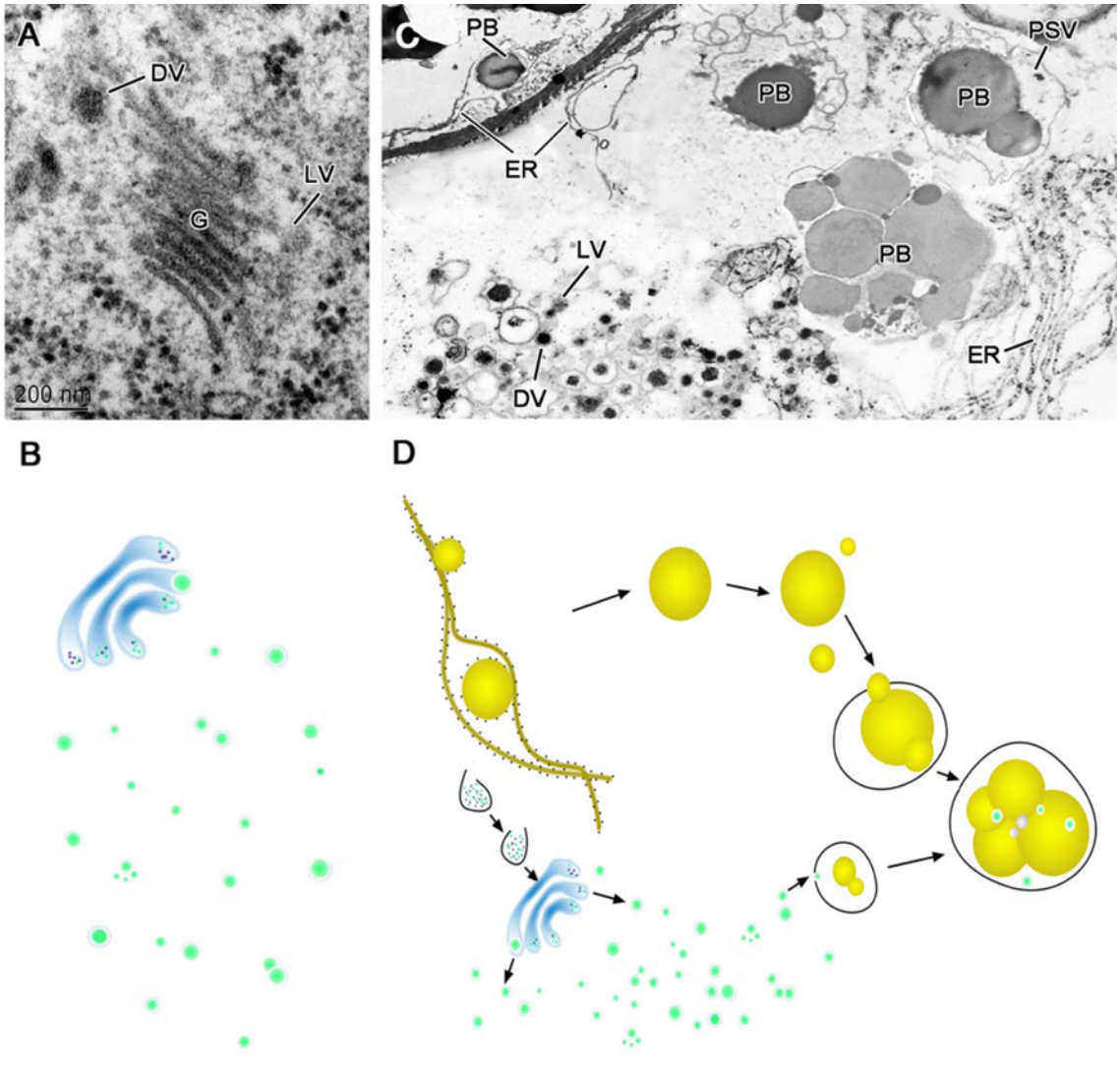

Fig. 10. Pathways of PBs formation in wheat endosperm cells. (A) Before 7 DPA, the Golgi apparatus produced electron-lucent vesicles and dense vesicles; (B) Before 7 DPA, the pattern of PBs formation; (C) After 7 DPA, the formation of PBs; (D) After 7 DPA, the pattern of PBs formation. SG, Starch granules; PB, Protein body; DV, Dense vesicles; LV, Lucent vesicles; ER, Endoplasmic reticulum; G, Golgi apparatus; PSV, protein storage vacuole.

DPA, the PBs changed from spherical to an irregular shape. At 18 DPA, the PBs gathered and protruded apparently. From 24 DPA, individual PBs was no longer visible, but a protein matrix was confined in the space between starch granules. These results are consistent with previous studies (Bechtel et al. 1982b; Loussert et al. 2008).

Wheat endosperm as a highly differentiated tissue contains specialized organelles for the accumulation of storage proteins (Tosi et al. 2009), which are ultimately deposited in PSV either derived from the ER or Golgi apparatus. Based on electron microscopic observations, we plotted the possible pathways of PBs formation in wheat endosperm (Fig. 10). At 7 DPA, there were abundant ER and the Golgi apparatus in the cells. A number of electron-lucent vesicles and dense vesicles were generated around the Golgi apparatus, while no PBs was observed in the ER. Bechtel (1982a) demonstrated the presence of PBs in Golgi dense vesicles by protease digestion. These protease-digested PBs occur near the Golgi apparatus at approximately 6 to 7 DPA. After 7 DPA, The Golgi apparatus were observed only very rarely in endosperm cells. While it is possible that Golgi appeared to lost most of their structural organization at later stages, but their structures were still present (Parker et al. 1982). PBs was synthesized in the ER. Mature PBs fell off the ER, fused and merged into the PSV. At the same time, the ER formed vesicles that were surrounded by Golgi vacuoles, electron-lucent vesicles and dense vesicles. In this case, the coat protein complex II played an important part in transporting proteins from ER to Golgi (Xu et al. 2016).

Enlargement of the small PBs near the Golgi apparatus

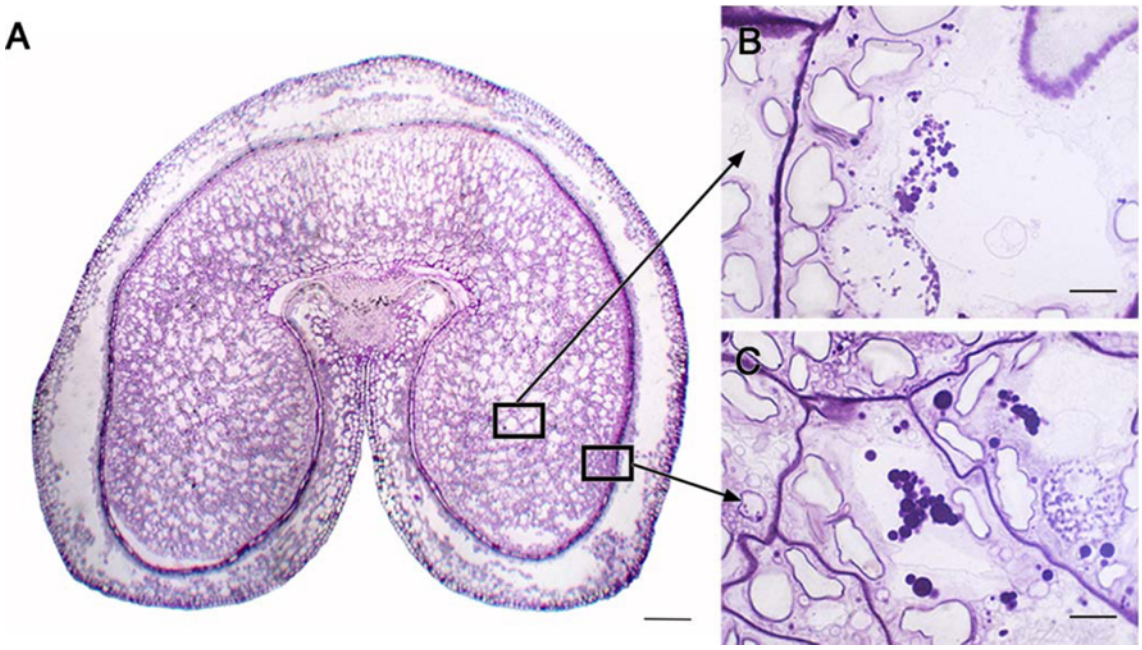

Fig. 11. (A) Micrographs of the transverse section of wheat caryopsis at 9 DPA. (B) the central region and (C) sub-aleurone region of endosperm. Bars = 50 μm in A; Bars = 10 μm in B–C.

occurred by two major mechanisms: one is fusion with one or more of the dense Golgi vesicles or electron-lucent Golgi-derived vesicles; another is fusion with other PBs at later stages of grain development. Loussert et al. (2008) proved that Golgi apparatus participated in the transport of gliadin and glutelin from the ER to the Golgi apparatus using immuno-localization. The ER probably transmitted proteins to the Golgi apparatus in the form of vesicles. Golgi apparatus secreted dense vesicles which gradually entered into vacuoles and fused with the PBs synthesized by the ER. Finally, the dense vesicles and PBs coexisted in the PSV.

It was discussed that gluten proteins accumulate within the ER while others pass via the Golgi apparatus to the vacuole. Muench et al. (1998) indicated that prolamin mRNA localization resulted from binding to a specific site on the tubulin and actin cytoskeleton. Rubin et al. (1992) advocated that some PBs was transported directly to vacuoles because the size is too large to enter the Golgi apparatus. This route may operate in concert with the known Golgi-mediated transport to vacuoles in which the storage proteins apparently condense into PBs at an ER location. Gliadin and globulin were retained within the ER lumen not by peptide signals but, rather, by aggregation, to form intracisternal inclusion granules known as PBs (Shewry et al. 1995). The accumulation of storage protein aggregates within the ER lumen must somehow bypass the unfolded protein response (UPR) pathway (Vitale et al. 2004).

Spatial Distribution Characteristics of Storage Protein

The PBs concentration was greater in the endosperm cells closest to the aleurone layer and decreased towards the center of endosperm (Savill et al. 2018). Similar result was observed in the present study. Based on the observation of morphology and structure of wheat caryopsis, Tosi et al. (2011) suggested that the quantitative and qualitative gradients in protein composition not only result from the origin of sub-aleurone cells but could also due to the action of specific regulatory signals on specific domains of the gluten protein gene promoters. In addition, Yu et al. (2015a) and Chen et al. (2016) demonstrated that the spatial distribution characteristics of protein may due to the nutrient transported pathways. The central endosperm, located downstream of the nutrient transport route, obtained less nutrition than the sub-aleurone. These studies could explain why the PBs in sub-aleurone layer were larger and more numerous compared with central endosperm region.

The main storage proteins accumulated during the grain filling are gliadin and glutenin. The cells of the central endosperm clearly contained HMW-GS but very little or no gliadin, this segregation may be retained even after PBs fusion and matrix formation (Tosi et al. 2009), but the LMW-GS and some gliadins more abundant in the sub-aleurone (Tosi et al. 2011). In this study, two kinds of PBs were observed in wheat endosperm: low-density PBs and high-density PBs. Gliadins existed mainly in low-density PBs at the early stage of grain development. At the later stage, both low-density and high-density PBs contained gliadin, while HMW-GS mainly existed in high-density PBs (Rubin et al. 1992). Zheng et al. (2018) found that HMW-GS accounted for the largest effect of nitrogen application on grain storage proteins factions, which resulted in pronounced variation in

wheat processing quality. Chope et al. (2014) demonstrated that the proportion of LMW-GS decreased during grain development and in response to nitrogen treatment and the proportion of total protein present in polymers in the mature grain decreased with increasing nitrogen level. Stoger et al. (2001) showed that the promoter of a LMW-GS gene conferred strong expression of the GUS reporter gene in the sub-aleurone and outer endosperm cell layers of developing seeds when used to transform wheat.

Development of PBs in Endosperm and the Response to Nitrogen

Nitrogen supply affected the synthesis and deposition of PBs. High-nitrogen supply significantly promoted starch granule and PBs during grain development (Kichey et al. 2007), especially resulting in the increment of proline content and glutamine synthetase activity in grains (Sun et al. 2013). Yu et al. (2017) indicated that nitrogen treatment affected key processes of protein biosynthesis such as mRNA processing and transport, amino acid biosynthesis and metabolism, aminoacyl-tRNA biosynthesis, ribosome biosynthesis and translation, protein export into RER, protein processing in the ER, ER-derived PBs formation, COP II vesicle-mediated protein transport, protein classification and packaging in Golgi, and PSV formation and PBs formation according to RNA-Seq data. Zheng et al. (2018) found that ER responded to nitrogen starvation by up-regulation of PDI, BiP and small heat shock proteins family, thereby enhancing the processing and accumulation of grain storage proteins. Ribosomal structure located at ER might change with nitrogen supply in grains, which may have some influences on the ER-drived route. This was consistent with our ultrastructural photographs, which revealed that the ER, Golgi apparatus and mitochondrion are more abundant at the early stage after nitrogen treatment. In addition, nitrogen also advanced the accumulation of PBs at the later stage. In the same period, the PBs of CG were small and dispersive, whereas the NTG was distributed in the form of larger protein aggregates. Due to the rapid accumulation rate of NTG PBs, endosperm cells were often aggregated and concentrated, whereas the PBs in the CG were mainly small PBs with slow accumulation rate. The PBs concentration of CG and NTG all showed a decreasing trend from the sub-aleurone to the center part, especially for albumin and globulin (Li et al. 2016).

Great differences in protein transcription and expression noted among wheat grain under different nitrogen supply. Transcript abundance reached a maximum at 21 DPA, being 3 to 4-fold greater under nitrogen application 200 and 350 kg hm^{-2} compared with 100 kg hm^{-2}. However, the effect of nitrogen treatment was less at 35 DPA (Wan et al. 2014). There was evidence of positive correlations among protein, Fe and Zn concentrations among diverse wheat cultivars (Xue et al. 2014). Increased nitrogen supply induced larger sink in the grain for Fe and Zn. And also, Zhen et al. (2017) found that enhanced enzyme activity from high-nitrogen application led to significant improvements in starch content, grain yield, and ultimately, bread making quality. Therefore, more work will be needed to elucidate the molecular and physiological mechanism of wheat protein development response to nitrogen treatment.

Materials and Methods

Plant Materials and N Treatment

Wheat (cvs. Ningmai 13) were planted at the experimental field of Yangzhou University with the density of 2.4×10^6 seedlings per hectare. And the experimental field was separated into several individual spaces (4 × 5 m) by plastic inserted into soil for stable nutrition concentration between the control and exogenous application of nitrogen.

The sandy loam soil contained organic substances (2.45%), nitrogen (106 mg kg^{-1}), phosphorus (33.8 mg kg^{-1}), and available potassium (66.4 mg kg^{-1}). The average annual temperature in this region was 15.2°C and the annual rainfall was 960 to 1044 mm. For the experiment, 240 kg N hm^{-2} of nitrogen (urea 46.67%) was used for NTG at booting stage. For the CG, no additional nitrogen was applied to the soil during the whole growth period. During flowering, individual floret was marked to accurately confirm caryopses stage by black pen at the spikelet bases (middle of the spikes). The wheat caryopses in different stages were collected for further analysis.

Preparation of Materials for Light Microscopy

Wheat caryopses at different developmental stages were transversely cut into 2 mm slices from the middle by razor blade. The caryopsis slices were immediately soaked in 2.5% glutaraldehyde fixative for 48 h. The fixed samples were subsequently washed by PBS (three times) and dehydrated in a graded ethanol series [20%, 40%, 60%, 80%, 90%, 95%, and 100% (thrice)], followed by propylene oxide replacement. Afterward, the samples were infiltrated and embedded in low-viscosity Spurr's resin and polymerised at 70°C. Then, they were cut into 1 μm slices using an ultramicrotome (Ultracut R, Leica, Germany) and pasted onto glass slides. Finally, the slices were stained with 0.5% methyl violet, rinsed, dried, and observed under a light microscope (DMLS, Leica, Germany). Each treatment selected three caryopses as repeats.

Specimen Processing for Transmission Electron Microscopy (TEM) Observation

The embedded sections used in resin slice were further trimmed. The tissues were sectioned about 70 nm thickness with a diamond knife on a Leica Ultracut R (Germany). The sections were collected on carbon-coated copper grids, fixed in a lead citrate solution for 30 min and then stained with uranyl acetate for 20 min. The sections were observed and photographed with the transmission electron microscope (Tecnai 12, Philips, Netherlands).

Calculation of PBs Number and Relative Area

Microscope images were obtained from the digital camera. Image-Pro Plus (ver. 6.0, Media Cybernetics, USA) and Photoshop (ver.

CS4, Adobe, USA) were used to calculate the number and relative area of PBs in sub-aleurone region and central endosperm region (Fig. 11) as previously described (Yu et al. 2015b). Data were tested using SPSS software (Version 19.0, International Business Machines Corporation, USA). The means were compared using Fisher's protected least at a probability significance level of $P<0.05$. Each treatment selected three caryopses as repeats, from which nine microscope images were randomly counted for each stage.

Protein Content Determination

Fresh wheat caryopses at different DPA were processed green removing treatment under 105°C for 1 h, dried to a constant weight in a ventilated oven under 42°C. The samples was then completely ground using a mortar and the powder was filtered through a 100 mesh wire screen. Up to 200 mg of the sample was mixed with the catalyst ($CuSO_4 + K_2SO_4$). The nitrogen content (%) was determined on an automatic Kjeldahl apparatus (FOSS KjeltecTM8400, Analyzer, Unit, Hoganas) after digesting the concentrated sulfuric acid. Storage protein content (%) was calculated using the nitrogen content value and multiplying it by the coefficient of 5.7. Three independent biological determinations were used for each sample.

Acknowledgements

The research was supported by the Natural Science Foundation (31571573, 31701351), a Project Funded by the Priority Academic Program Development of Jiangsu Higher Education Institutions (PAPD).

Author's Contributions

FX, XY and YY conceived the experiment; ZD participated in collecting wheat samples in different stages; YY, XC performed the experiment; YY, LR and YW analyzed the data; YY wrote the manuscript; FX critically revised the manuscript. The authors declare that they have no conflicts of interest.

References

Arcalis E, Marcel S, Altmann F, Kolarich D, Drakakaki G, Fischer R (2004) Unexpected deposition patterns of recombinant proteins in post-endoplasmic reticulum compartments of wheat endosperm. Plant Physiol 136:3457–3466

Bechtel DB, Gaines RL, Pomeranz Y (1982a) Early stages in wheat endosperm formation and protein body initiation. Ann Bot-London 50:507–518

Bechtel DB, Gaines RL, Pomeranz Y (1982b) Protein secretion in wheat endosperm-formation of the matrix protein. Cereal Chem 59:336–343

Chen XY, Shao SS, Wang LL, Zhu XW, Yang Y, Wang WJ, Yu XR, Xiong F (2016) Accumulation characteristic of protein bodies in different regions of wheat endosperm under drought stress. J Integr Agr 15:2921–2930

Chope GA, Wan Y, Penson SP, Bhandari DG, Powers SJ, Shewry PR, Hawkesford MJ (2014) Effects of genotype, season, and nitrogen nutrition on gene expression and protein accumulation in wheat grain. J Agr Food Chem 62:4399–4407

Don C, Mann G, Bekes F, Hamer RJHF (2006) HMW-GS affect the properties of glutenin particles in GMP and thus flour quality. J Cereal Sci 44:127–136

Galili G, Altschuler Y, Levanony H, Giorinisilfen S, Shimoni Y, Shani N (1995) Assembly and transport of wheat storage proteins. J Plant Physiol 145:626–631

Garcíamolina MD, Barro F (2017) Characterization of changes in gluten proteins in low-gliadin transgenic wheat lines in response to application of different nitrogen regimes. Front Plant Sci 8: 257

Guo G, Lv D, Yan X, Subburaj S, Yan Y (2012) Proteome characterization of developing grains in bread wheat cultivars (*Triticum aestivum* L.). BMC Plant Biol 12:147

Iqtidar H, Ayyaz KM, Ahmad KE (2006) Bread wheat varieties as influenced by different nitrogen levels. J Zhejiang Unvi-Sc B 7: 72–80

Katarzyna D, Ewa F, Lidia S (2018) Expression of genes encoding protein disulfide isomerase (PDI) in cultivars and lines of common wheat with different baking quality of flour. BMC Plant Biol 18: 294

Kichey T, Hirel B, Heumez E, Dubois F, Gouis JL (2007) In winter wheat (*Triticum aestivum* L.), post-anthesis nitrogen uptake and remobilisation to the grain correlates with agronomic traits and nitrogen physiological markers. Field Crop Res 102:22–32

Kim WT, Franceschi VR, Okita KTW (1988) Formation of wheat protein bodies: involvement of the golgi apparatus in gliadin transport. Planta 176:173–182

Kumamaru T, OgawaM, Satoh H, Okita TW (2007) Protein body biogenesis in cereal endosperms. Plant Cell Monographs 8:141–158

Li C, Xu Z, Dong Z, Shi S, Zhang J (2016) Effects of nitrogen application rate on the yields, nutritive value and silage fermentation quality of whole-crop wheat. Asian-Austral J Anim 29:1129–1135

Li XN, Zhou LJ, Liu FL, Zhou Q, Cai J, Wang X, Dai TB, Cao WX and Jiang D (2016) Variations in protein concentration and nitrogen sources in different positions of grain in wheat. Front Plant Sci 7:942

Loussert C, Popineau Y, Mangavel C (2008) Protein bodies ontogeny and localization of prolamin components in the developing endosperm of wheat caryopses. J Cereal Sci 47:445–456

Martre P (2003) Modeling grain nitrogen accumulation and protein composition to understand the sink/source regulations of nitrogen remobilization for wheat. Plant Physiol 133:1959–1967

Moore KL, Tosi P, Palmer R, Hawkesford MJ, Grovenor CRM, Shewry PR (2016) The dynamics of protein body formation in developing wheat grain. Plant Biotechnol J 14:1876–1882

Muench DG, Wu Y, Coughlan SJ, Okita TW (1998) Evidence for a cytoskeleton-associated binding site involved in prolamine mRNA localization to the protein bodies in rice endosperm tissue. Plant Physiol 116:559−569

Normand FL, Hogan JT, Deobald HJ (1965) Protein content of successive peripheral layers milled from wheat, barley, grain sorghum, and glutinous rice by tangential abrasion. Cereal Chem 42:359–367

Parker ML (1982) Protein accumulation in developing endosperm of a high protein line of *Triticum dicoccoides*. Plant Cell Environ 5:37–43

Rubin R, Levanony H, Galili G (1992) Evidence for the presence of two different types of protein bodies in wheat endosperm. Plant Physiol 99:718–724

Savill G, Michalski A, Powers SJ, Wan Y, Tosi P, Buchner P (2018) Temperature and nitrogen supply interact to determine protein distribution gradients in the wheat grain endosperm. J Exp Bot 69:3117–3126

Shewry PR, D'Ovidio R, Lafiandra D, Jenkins J A, Mills ENC, Békés F (2009) Wheat grain proteins. Wheat Chemistry Technology 223–298

Shewry PR, Napier JA, Tatham AS (1995) Seed storage proteins:

structures and biosynthesis. Plant Cell 7:945–956
Stoger E, Parker M, Christou P, Casey R (2001) Pea legumin overexpressed in wheat endosperm assembles into an ordered paracrystalline matrix. Plant Physiol 125:1732–1742
Sun M, Gao Z, Zhao W, Deng L, Deng Y, Zhao H, Ren A, Li G, Yang Z (2013) Effect of subsoiling in fallow period on soil water storage and grain protein accumulation of dryland wheat and its regulatory effect by nitrogen application. PloS One 8:e75191
Tosi P (2012) Trafficking and deposition of prolamins in wheat. J Cereal Sci 56:81–90
Tosi P, Gritsch CS, He J, Shewry PR (2011) Distribution of gluten proteins in bread wheat (*triticum aestivum*) grain. Ann Bot-London 108:23–35
Tosi P, Parker M, Gritsch CS, Carzaniga R, Martin B, Shewry PR (2009) Trafficking of storage proteins in developing grain of wheat. J Exp Bot 60:979–991
Vensel WH, Tanaka CK, Altenbach SB (2014) Protein composition of wheat gluten polymer fractions determined by quantitative two-dimensional gel electrophoresis and tandem mass spectrometry. Proteome Sci 12:8
Vitale A, Ceriotti A (2004) Protein quality control mechanisms and protein storage in the endoplasmic reticulum. A conflict of interests? Plant Physiol 136:3420–3426
Wan Y, Gritsch CS, Hawkesford MJ (2014) Effects of nitrogen nutrition on the synthesis and deposition of the -gliadins of wheat. Ann Bot-London 113:607–615
Wang YF, Jiang D, Yu ZW, Cao WX (2003) Effects of nitrogen rates on grain yield and protein content of wheat and its physiological basis. Scientia Agricultura Sinica 36:513–520
Wu XJ, Li WX, Hu SL (2005) Accumulation pattern of gliadin fractions α, β, γ, ω and regulation of nitrogen. Scientia Agricultura Sinica 38:741–746
Xu XF, Pu XJ, Mo BX (2016) Functions of copii subunits in protein secretory pathway. Chinese Bulletin of Life Sciences 28:442–451
Xue YF, Eagling T, He J, Zou CQ, Mcgrath SP, Shewry PR, Zhao FJ (2014) Effects of nitrogen on the distribution and chemical speciation of iron and zinc in pearling fractions of wheat grain. J Agr Food Chem 62:4738–4746
Yang M, Dong J, Zhao W, Gao X (2016) Characterization of proteins involved in early stage of wheat grain development by itraq. J Proteomics S1874391916300070
Yu XR, Chen XY, Wang LL, Yang Y, Xiong F (2017) Novel insights into the effect of nitrogen on storage protein biosynthesis and protein body development in wheat caryopsis. J Exp Bot 68: 2259–2275
Yu XR, Yu H, Shao SS, Zhang J, Zhou L, Zheng YK, Xiong F, Wang Z (2015a) Structural development of conducting cell and its functions in wheat caryopsis. Braz J Bot 38:401–409
Yu XR, Zhou L, Zhang J, Yu H, Xiong F, Wang Z (2015b) Comparison of starch granule development and physicochemical properties of starches in wheat pericarp and endosperm. J Sci Food Agr 95: 148–157
Zhen S, Deng X, Zhang M, Zhu G, Lv D, Wang Y, Zhu D, Yan Y (2017) Comparative phosphoproteomic analysis under high-nitrogen fertiliser reveals central phosphoproteins promoting wheat grain starch and protein synthesis. Front Plant Sci 8:67